

A study on the low-latitude daytime *E* region plasma irregularities using coordinated VHF radar, rocket-borne, and ionosonde observations

A. K. Patra,¹ N. Venkateswara Rao,¹ D. V. Phanikumar,^{1,2} H. Chandra,³ U. Das,³ H. S. S. Sinha,³ T. K. Pant,⁴ and S. Sripathi⁵

Received 11 June 2009; accepted 20 July 2009; published 3 November 2009.

[1] In this paper we study the off-electrojet low-latitude daytime *E* region plasma irregularities using first multi-instrument observations in India made during July 2004 by the MST radar from Gadanki (13.5°N, 79.2°E, magnetic latitude 6.4°N), Langmuir probe on board the RH-300 Mk II rocket, and ionosonde from Sriharikota (13.6°N, 80.2°E, magnetic latitude 6.4°N). Radar echoes were confined to altitudes below 105 km and were observed in the form of a descending echoing layer with the descent rate of 1 km/h. Virtual height of the *E* layer, as observed by ionosonde, shows identical descending behavior. A detailed analysis based on the radar and ionosonde observations shows that the radar echoes are related to the range spread in the ionogram. Rocket observations made on 23 July 2004 revealed weak plasma irregularities with scale sizes more than 100 m and no noticeable irregularity at shorter scales. The spectral slope of the irregularities observed by the rocket probe is found to be -4 for scales in between 1 km and 100 m. During the rocket launch, radar did not detect any echo conforming that the small-scale irregularities were not present. Examination of concurrent observations of neutral wind made by TIMED Doppler interferometry suggests that zonal wind plays a crucial role in forming electron density layers, which become unstable via the gradient drift instability with background electric field or/and zonal neutral wind generating low-latitude *E* region plasma irregularities.

Citation: Patra, A. K., N. Venkateswara Rao, D. V. Phanikumar, H. Chandra, U. Das, H. S. S. Sinha, T. K. Pant, and S. Sripathi (2009), A study on the low-latitude daytime *E* region plasma irregularities using coordinated VHF radar, rocket-borne, and ionosonde observations, *J. Geophys. Res.*, *114*, A11301, doi:10.1029/2009JA014501.

1. Introduction

[2] Off-electrojet low-latitude *E* region field-aligned-irregularities (FAIs) studied using the MST radar located at Gadanki (13.5°N, 79.2°E, magnetic latitude 6.4°N) have been found to occur round the clock [Patra *et al.*, 2004]. Radar observations made from a similar low-latitude location in the southern hemisphere Piura (5.2°S, 80.6°W, magnetic latitude 7°N), however, showed that the *E* region FAIs do not occur during the midday (1100–1400 LT) [Chau *et al.*, 2002].

[3] Radar observations made from both Gadanki and Piura, however, have displayed similar Doppler spectral characteristics and echoing morphology [Choudhary *et al.*, 1996; Patra *et al.*, 2004; Woodman *et al.*, 1999; Chau *et al.*, 2002]. The spectra are characterized as type 2 (representing

the presence of turbulent process). No type 1 spectrum has been observed yet. The general understanding is that the gradient drift instability is responsible for the generation of the *E* region FAIs associated with the type 2 spectra. The occurrence of radar echoes during the night, morning, and late afternoon suggests that electron density gradient, which often appears in the low background density, plays an important role and thus also indirectly supports the role of gradient drift instability as the governing mechanism.

[4] The Gadanki radar, however, often observes the *E* region FAIs during the midday. Krishnamurthy *et al.* [1998] surmised that the occurrence/nonoccurrence of daytime irregularities responsible for the radar echoes at Gadanki may be related to the presence/absence of blanketing sporadic *E* layer since they only can provide required electron density gradient during the midday for the growth of the gradient drift instability. Patra *et al.* [2005], however, did not find any close relation between the radar echoes and blanketing sporadic *E*. On the other hand, Raghavarao *et al.* [2002] argued that the day-to-day variation in the latitudinal distribution of the equatorial electrojet current system may be responsible for the occurrence/nonoccurrence of radar echoes at Gadanki during the midday. Thus identification of the free energy sources responsible for the daytime irregu-

¹National Atmospheric Research Laboratory, Gadanki, India.

²Now at Korea Astronomy and Space Science Institute, Daejeon, South Korea.

³Physical Research Laboratory, Ahmedabad, India.

⁴Space Physics Laboratory, VSSC, Trivandrum, India.

⁵Indian Institute of Geomagnetism, Navi Mumbai, India.

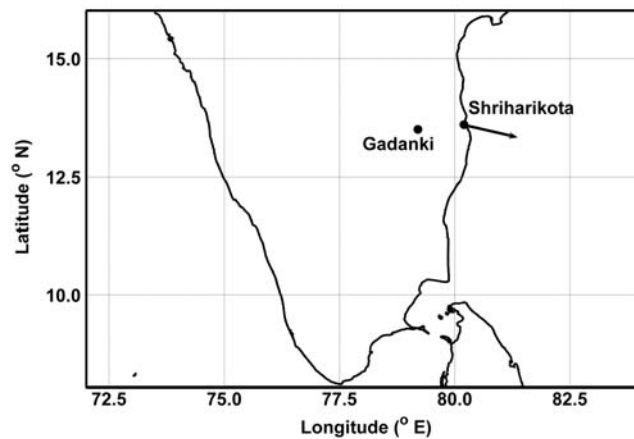


Figure 1. Map showing the locations of the MST radar at Gadanki and the rocket range at Sriharikota. The trajectory of the rocket is also shown.

larities and for the radar echoes at Gadanki still remains an open issue.

[5] We conducted coordinated observations using the Gadanki MST radar and rocket-borne electron density measurements from Sriharikota (13.6°N, 80.2°E, magnetic latitude 6.4°N), a rocket range located 110 km east of the radar site, to study the electron density fluctuations in the mesosphere and in the *E* region. A digital ionosonde located at Sriharikota was also operated during the campaign supporting the *E* region investigations. The mesospheric studies made using the campaign observations have been reported recently by *Chandra et al.* [2008]. In this paper, we present and discuss the daytime observations of the low-latitude *E* region FAIs made by the Gadanki MST radar in the light of simultaneous observations of electron density fluctuations and *E* layer characteristics.

2. Experiment Description

[6] A RH-300 Mk II rocket carrying a Langmuir probe (LP) payload and an RH-200 rocket carrying metallic chaff payload were launched on 23 July 2004 from Sriharikota to study the electron density fluctuations in the mesosphere and in the *E* region. The RH-200 based observations of winds were limited to the height range of 20–76 km and thus will not be discussed any more in this paper. Gadanki radar observations were made during 22–27 July 2004. Ionosonde observations from Sriharikota were made on 22, 23, 26, and 27 July 2004. Figure 1 shows the locations of Gadanki and Sriharikota and the trajectory of the RH-300 Mk-II rocket.

2.1. Radar Experiments

[7] The Gadanki MST radar was operated during daytime in the period of 22–27 July 2004 to study the characteristics of echoes from the mesosphere and the *E* region. The radar parameters used for the experiments are given in Table 1. Note that in addition to 5 beams (east, west, north, and south with look angle of 10° off zenith and a zenith beam) used for mesospheric investigations, we used a beam oriented at 13° off-zenith due north that satisfies perpendicularity to Earth's magnetic field at the *E* region altitudes

and detects the backscattered echoes from the FAIs. Power spectral data covering 60–120 km range with a range resolution of 450 m were obtained. Owing to the use of number of beams, we could obtain *E* region observations every 67 s. It may be noted from Table 1 that 40 pulse returns were integrated to increase the signal-to-noise ratio of the mesospheric echoes. This fixed the unambiguous velocity limit at $\pm 39.3 \text{ m s}^{-1}$. It may be mentioned that for the *E* region echoes, while a larger unambiguous velocity limit than that used in the present experiments (i.e., $\pm 39.3 \text{ m s}^{-1}$) is required to avoid velocity aliasing, a compromise was made considering the poor signal strength and narrowness of the mesospheric spectra in mind. The occurrence and strength of the *E* region echoes, which are of primary concern here, however, are not affected by the limited Doppler window used in these experiments. We computed signal-to-noise ratio (SNR) using the noise power reckoned over the entire observational Doppler window of $\pm 39.3 \text{ m s}^{-1}$.

2.2. RH-300 Mk-II Rocket Experiment

[8] The rocket was launched at 1142 LT on 23 July 2004. The rocket nose cone was ejected at 60 km and the rocket reached an apogee of 109 km. A fixed bias LP, similar to the one described by *Prakash and Subbaraya* [1967] was used to measure electron density fluctuations. The LP sensor was a split sphere (50 mm diameter), whose upper hemisphere was biased at +4 V and was used to collect the electron current, and the lower hemisphere was used as a guard electrode. The LP sensor was mounted on the top deck of the RH-300 MK II rocket using a 200 mm long boom. To cover the large dynamical range of current due to variation in the electron density in the mesosphere to the *E* region, an automatic gain-change amplifier was used to measure the current in the range of 1 nA to 3 μA . For studying the electron density fluctuations in different scale sizes, the current collected by the LP sensor was processed onboard in three channels with different gains having frequency response of 0–100 Hz, 30–150 Hz, and 70–1000 Hz. These channels were sampled at 520 Hz, 1040 Hz, and 5200 Hz, respectively. The consolidated wave number power spectrum of the irregularities was constructed from the electron density fluctuations obtained from these three channels. For the first two channels and the last two channels, normalization was done at 50 Hz and 100 Hz, respectively. With the knowledge of the rocket velocity in the region of interest, the spectrum, therefore, gives infor-

Table 1. Radar Parameters Used for the Experiments

Parameter	Value
Frequency	53 MHz
Peak Power-Aperture product	$3 \times 10^{10} \text{ W m}^2$
Beam (3 dB)	3°
Beam directions	E, W, Z, N, S, 13°N
Receiver bandwidth	1.7 MHz
Interpulse period (IPP)	0.9 ms
Pulse width	3 μs
Number of coherent integrations	40
Number of FFT points	256
Range coverage	60–120 km
Range resolution	450 m
Nyquist velocity limit	$\pm 39.3 \text{ m s}^{-1}$
Velocity resolution	0.3 m s^{-1}

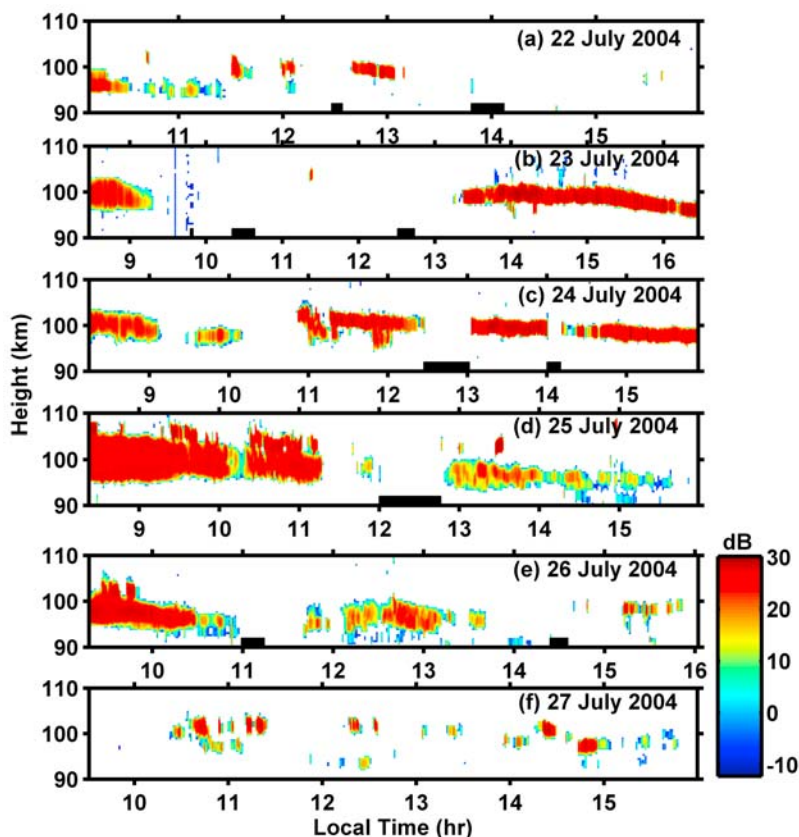


Figure 2. Height time variation of SNR of the E region echoes observed during 22–27 July 2004.

mation about the irregularity scale sizes. Fast Fourier transform with Hanning window was used to estimate the power spectrum.

2.3. Ionosonde Experiments

[9] A digital ionosonde (IPS-42) located at Sriharikota was operated on 22, 23, 26, and 27 July and ionograms at every 15 min (5 min for sometime on 22 and 23 July) interval were recorded. The virtual height ($h'E_s$), the top frequency reflected/scattered (f'_iE_s), and the blanketing frequency (f_bE_s) of the E_s layer were derived for comparing them with the radar observations.

3. Observations

3.1. Radar Observations

[10] Figures 2a–2f show the height-time variation of SNR of the radar echoes observed during 22–27 July 2004. Echo height is obtained by multiplying $\text{Cos } 13^\circ$ ($= 0.974$) by the echo range. The height ambiguity could be 550 m as estimated by *Patra et al.* [2002]. The horizontal thick bars represent data gaps arising due to nonoperation of the radar at those times. The fact that the echoes were observed on all the 6 days indicates that the daytime echoes are regularly observed, which is consistent with the earlier finding [*Patra et al.*, 2004]. Note that the echoes, however, were not observed continuously on any given day, suggesting the lack of free energy at times for generating small-scale irregularities. The echoes were observed mostly below 105 km and the echoing layers clearly show descending

pattern reminiscent of the tidal wind behavior. The average descent rates are close to 1 km/h. Echo SNR is found to be as high as 30 dB. SNR of -10 dB is found to correspond to noise-like echoes. This implies that the dynamic range of echo SNR is 40 dB. Echoes having SNR of 30 dB can be considered as strong and compare well with those reported as strong signals based on large statistical data by *Patra et al.* [2004]. It is important to note that radar echoes were not observed during 0920–1320 LT on 23 July and the rocket was launched at 1142 LT on this day from Sriharikota. Before 0920 LT and after 1320 LT, echo SNRs, however, were consistently high with values as high as 30 dB. Although echoes were not observed during the rocket flight, we will show later that the results obtained from the radar, rocket and ionosonde observations provided very useful information in understanding the radar echoes from the daytime E region.

3.2. Rocket Observations

[11] Figures 3a and 3b show the electron density profile and inverse density gradient scale lengths, $L^{-1} = [(1/n_e)(dn_e/dh)]$, respectively, measured during the upleg. The L^{-1} values were calculated over an altitude interval of 200 m. Note that the peak electron density of 1.8×10^5 electrons/cm³ was observed at 98 km. Also note that the L^{-1} values were less than 0.5 km^{-1} , representing weak density gradient.

[12] Figure 4 shows the frequency spectrum of the electron density fluctuations observed between 98.8 and 100.5 km during the upleg. Note the top scale, which represents the scale sizes of the irregularities. The spectral

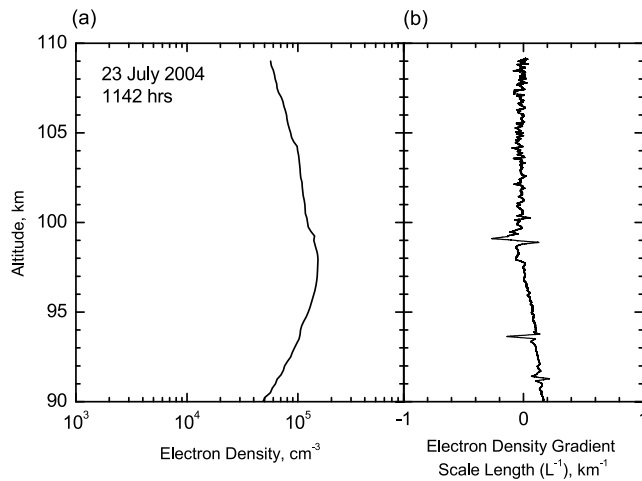


Figure 3. Height profiles of (a) electron density and (b) inverse of the electron density gradient scale length observed during the upleg.

slopes represented by the slant solid lines are -4 for scales in between 1 km and 100 m and -0.18 for scales below 100 m. Notably, irregularities with scale sizes less than 100 m are all noise-type and thus have no significance. We may recall that the powerful Gadanki radar did not detect echoes during the rocket launch although at other times it detected signals with SNR as high as 30 dB. Thus the absence of meter-scale irregularities in the rocket observations and the absence of radar echoes are consistent with each other. Later, we will discuss these results in detail.

3.3. Ionosonde Observations

[13] *Patra et al.* [2005] have already shown that the radar echoes are not related to $f_b E_s$. Thus we focus on presenting the variations in $h' E_s$, $(f_i E_s - f_b E_s)$ and a few ionograms to compare them with the radar and rocket observations. Considering the low latitude of Sriharikota, we consider the $(f_i E_s - f_b E_s)$ values as tracers of spatial inhomogeneity in electron density [*Maruyama et al.*, 2006].

[14] Figures 5a and 5b show time variations of $h' E_s$ and $(f_i E_s - f_b E_s)$, respectively, observed on 22, 23, 26, and 27 July. Data gaps represent nonavailability of ionosonde observations due to power failure. From Figure 5a, one can clearly see the descending trends of the E_s layers with the descent rate of 1 km/h, which is close to the descent rate of diurnal tidal wind node. On 27 July, large variations observed in the height of the layer appear to be related to reflection of HF waves from two distinctly different layers separated in height, not due to fast ascent or descent of an E_s layer. In the case of a horizontally moving ionospheric E region, if the density in the lower layer has spatial variability, it would allow the HF waves to get reflected from the top layer. Accordingly, one would expect unusual change in the layer height. This is an inference based on the multiple radar echoing regions observed on 27 July unlike that observed on other days. Note that the virtual heights of the E_s layers are higher than the altitude region of the radar echoes. This difference is expected during daytime due to group retardation of the

HF waves owing to the electron density below the E region.

[15] Figure 5b illustrates the variations in $f_i E_s - f_b E_s$. Most of the values are less than 3 MHz except for 23 July during 1300–1400 LT (observations after 1400 LT are not available). Also, values less than 0.5 MHz (half of the gyrofrequency, which is ~ 1 MHz) should be disregarded since such a difference could come from echoes related to extraordinary and ordinary waves. When the radar observations are compared with the $(f_i E_s - f_b E_s)$ values, we find no one-to-one relation between them. For example, on 23 July, radar echoes were equally strong in the morning and afternoon corresponding to which the $(f_i E_s - f_b E_s)$ values are vastly different. $(f_i E_s - f_b E_s)$ is < 3 MHz before 0900 LT, while it is as high as 6 MHz after 1300 LT. Also echoes on 26 July before 1130 LT are strong, but $(f_i E_s - f_b E_s)$ values are < 3 MHz. A contrasting feature can be observed on 27 July, where the radar echoes are relatively weak and discontinuous, but the $(f_i E_s - f_b E_s)$ values in general are more than those of 23 and 26 July.

[16] In order to understand better the ionogram observations in terms of off-electrojet daytime irregularities and to relate them to the radar and rocket observations, we present a few sets of ionogram taken at different times on different days in Figures 6 and 7. Figure 6a shows the ionogram observed at 1142 LT on 23 July (the time of rocket launch). While, the maximum frequency reflected/scattered from the E region is found to be 4.5 MHz, the blanketing frequency is 3.8 MHz, which corresponds to an electron density of 1.8×10^5 electrons/cm³. No echo is observed at frequencies below 2.2 MHz. Note that there is no noticeable range spread in the ionogram. Also we may recall that at this time, radar echoes were not observed, but rocket observations showed irregularities at scales larger than 100 m. Figures 6b and 6c show the ionograms observed

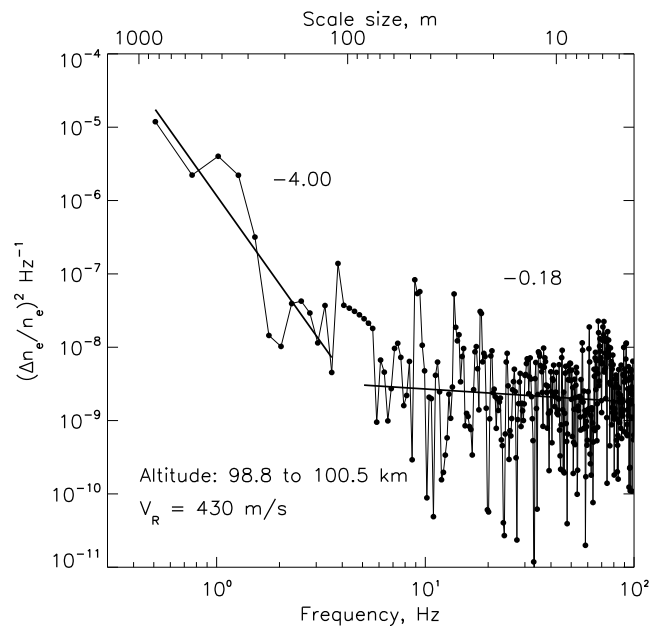


Figure 4. Wave number spectrum of electron density fluctuations observed for the height region 98.8–100.5 km during the upleg.

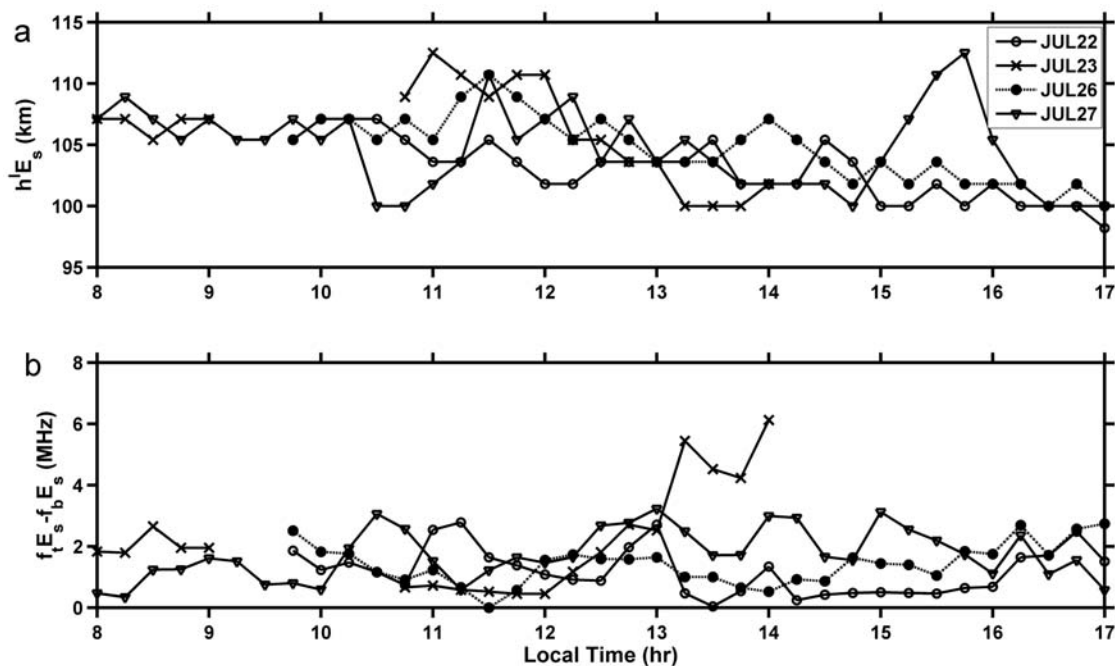


Figure 5. (a) Time variations of $h'E_s$ and (b) $(f_t E_s - f_b E_s)$ observed on 22, 23, and 27 July 2004. Different symbols represent observations made on different days. The data gaps represent the nonavailability of ionosonde data due to power failure.

on 23 July at 0845 LT and 1400 LT, respectively. They show range spread unlike that observed at 1142 LT (Figure 6a). At 1400 LT, however, both the peak frequency and blanketing frequency are larger than those observed at 0845 LT. Also, the ionogram observed at 1400 LT shows strong blanketing type ionization up to ~ 5 MHz and is characterized by triple reflection compared to that observed as double reflection at 0845 LT. We may recall that while at both the times, radar echoes were equally strong; the ionograms indicate that E_s activity was stronger at 1400 LT than at 0845 LT.

[17] In an effort to generalize whether the ionograms have any common feature that directly relates to radar echoes, we investigated the ionograms observed on different days. Figure 7a shows ionograms corresponding to 22 July (1200 LT), 26 July (0945 LT), and 27 July (1400 LT) when radar echoes were observed. Similarly, Figure 7b shows ionograms corresponding to 22 July (1500 LT), 26 July (1400 LT), and 27 July (1000 LT) when radar echoes were not observed. As is evident, ionograms corresponding to the presence of radar echoes show larger range spread than those observed in the absence of radar echoes. Also we find that $(f_t E_s - f_b E_s)$ and $f_t E_s$ values are larger in the former case than in the latter.

4. Discussion

[18] We have shown that E region echoes were observed on all the days and the echoing layers displayed descent rates of ~ 1 km/h. The E_s layers also showed similar descending features. Note that the descending behavior of the E_s layer is very different from those observed at the magnetic equator. At the magnetic equator, a forenoon descent and afternoon ascent is observed, which can be attributed to the solar zenith angle dependence of the

electron density layer. Thus the observed descending behavior of the E_s layers (descent rate of 1 km/h) can be attributed to the dynamical effect presumably due to diurnal tidal wind [Mathews and Bekey, 1979]. Similar descending trend observed in the radar echoing layer and in the E_s height thus suggests that electron density layering phenomenon is closely related to the occurrence of low-latitude radar echoes. We, however, have not found any close relationship between radar echoes and $(f_t E_s - f_b E_s)$. If we consider the large values of $(f_t E_s - f_b E_s)$ as an indicator of large-scale spatial structures in electron density, it appears that the continuous echoing layers occur when there is no large-scale spatial inhomogeneity in electron density. Coming to the link of radar echoes to the blanketing E_s , we found that when strong blanketing E_s , which is characterized by multiple reflections, is present, radar echoes are present, but vice versa is not true. Thus it is not clear as to how the $f_b E_s$ or $(f_t E_s - f_b E_s)$ are related to radar echoes.

[19] An important finding, not reported earlier for low-latitude observations, is the range spread in the E region ionogram that relates quite well with the radar echoes. We may mention here that for the nighttime continuous echoes from midlatitude E region, Maruyama *et al.* [2006] noticed some range spread in the E region ionograms. We expect to observe a clean trace in the ionogram having no range spread echoes if HF radio waves are purely reflected from E region plasma density. In such a case, $f_t E_s$ can be used to derive the critical plasma frequency (hence, plasma density) of the E region. Thus ionosonde observations showing range spread and having close correlation with the radar echoes clearly suggest that range spread ionograms represent the presence of plasma irregularities. In such cases, the $f_t E_s$ values need to be used carefully in terms of critical plasma frequency since some of the HF echoes may arise

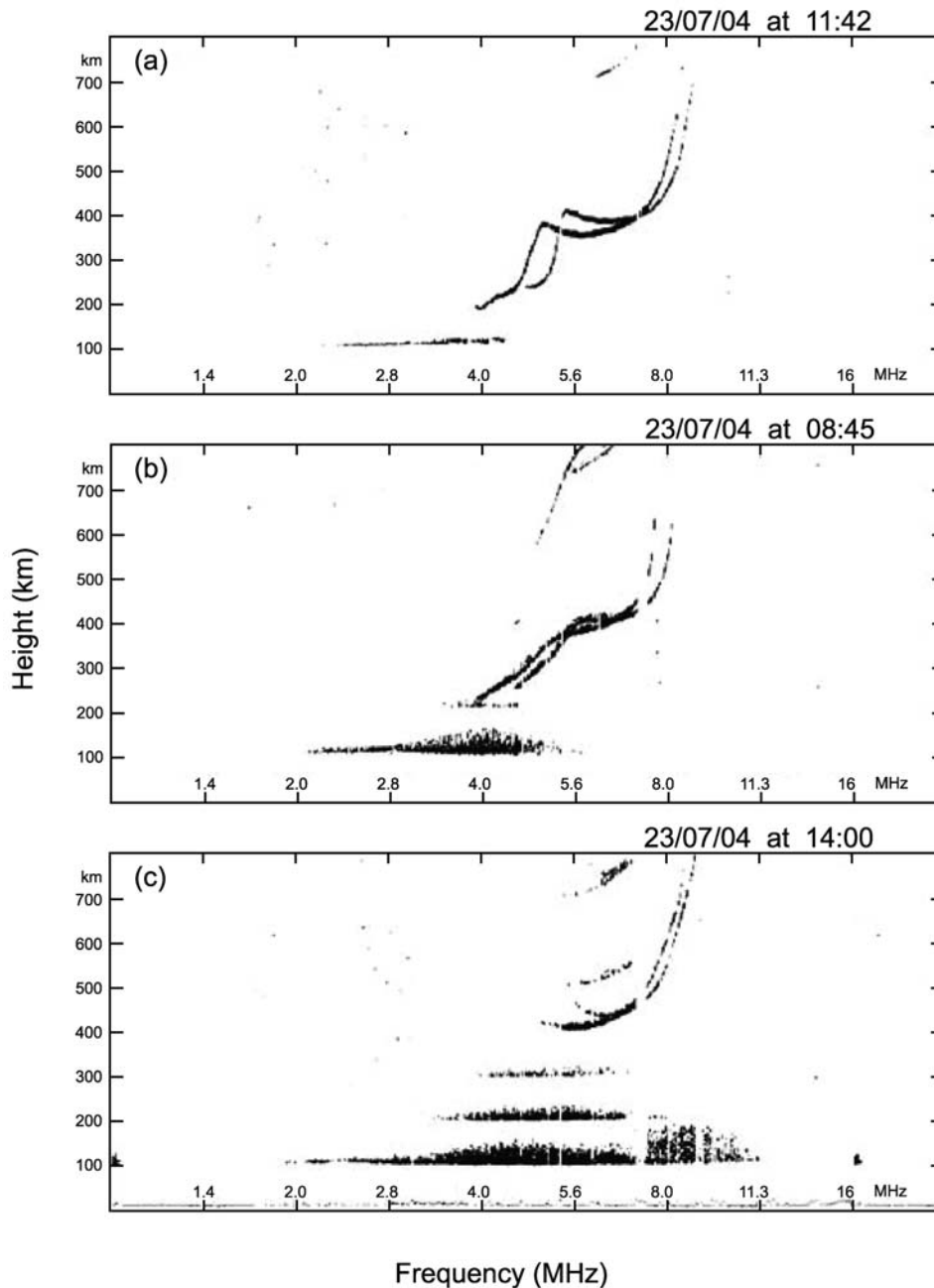


Figure 6. Ionograms observed on 23 July at (a) 1142 LT, (b) 0845 LT, and (c) 1400 LT.

due to scattering. Now, if we were to interpret the range spread ionograms as due to small-scale inhomogeneities in electron density, as discussed above, we have two possible explanations: (1) HF radio waves are scattered from oblique directions from the small-scale inhomogeneities owing to their different orientations, which would result in finite range spread in the ionogram and (2) HF radio waves penetrate deep into the *E* layer due to the porous nature of the irregular *E* layer wherein small-scale irregularities are also part of it. It is also known that while large-scale plasma blob structures do not occur at the magnetic equator unlike those at the low and middle latitudes, ionograms related to the equatorial electrojet show large range spread in connec-

tion with the electrojet irregularities. Thus the small range spread in the ionograms reported here can as well be regarded as due to equatorial-type plasma irregularities with albeit lower level of turbulence than that of the electrojet. In such a case, oblique scattering of radio waves from the irregularities would be able to account for the range spread echoes in the ionogram.

[20] Coming to the rocket observations, we found that irregularities with scale sizes >100 m only were present. The MST radar did not detect any echo during the rocket experiment. Interestingly, note that the height region of irregularities observed in the LP data and that of radar observations before 0920 LT and after 1320 LT is the same.

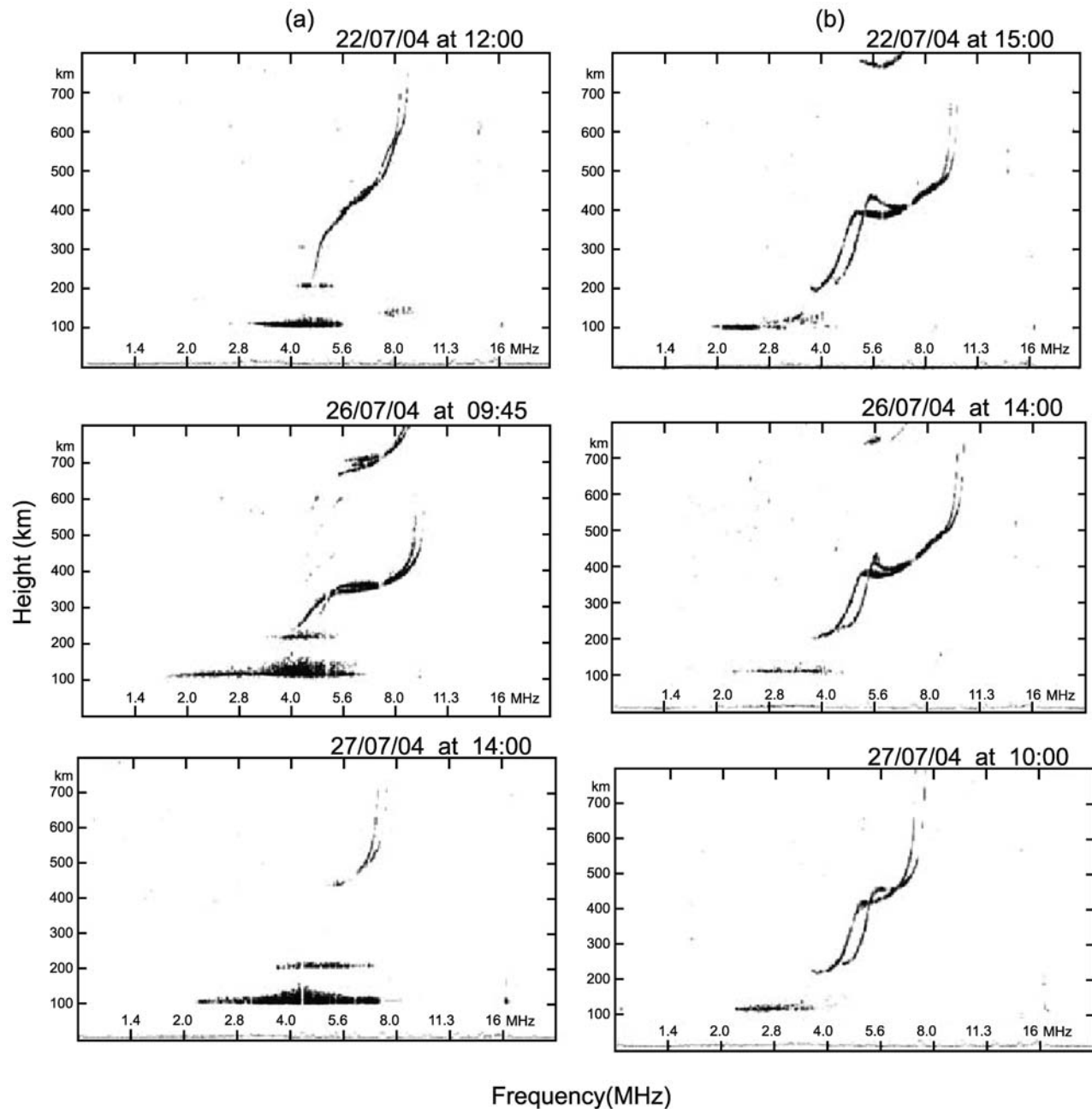


Figure 7. Ionograms observed on different days when (a) radar echoes were observed and (b) radar echoes were not observed.

It is also interesting to note that although weak electron density irregularities with scale sizes greater than 100 m (as observed by rocket probe) were present, they were not sufficient to produce range spread ionogram.

[21] In this context, the spectrum of the electron density irregularities assumes importance. The spectral slope is found to be -4 for irregularity scale sizes in between 1 km and 100 m, which is steeper than those reported as less than -3 by several investigators in the past [e.g., *Hysell et al.*, 1994; *Mori and Oyama*, 1998; *Kelley and Livingston*, 2003; *Kelley et al.*, 2004]. Also the spectral energies observed in the scale sizes of 100 m – 1 km are lower by

3–4 orders than that observed by others [e.g., *Hysell et al.*, 1994; *Kelley and Livingston*, 2003; *Kelley et al.*, 2004]. Moreover, the spectral energies at scales less than 100 m are insignificant. Coming to the detection of radar echoes, *Hysell et al.* [1994] observed strong VHF radar echoes in connection with rocket observations of electron density fluctuations that showed spectral slopes of -2.21 (in the upleg) and -1.95 (in the downleg) for scale sizes larger than ~ 50 m and -4.5 (in the upleg) and -5.03 (in the downleg) for scales shorter than ~ 50 m. Also, *Mori and Oyama* [1998] observed strong VHF radar echoes corresponding to the electron density fluctuations having spectral slopes of -0.8

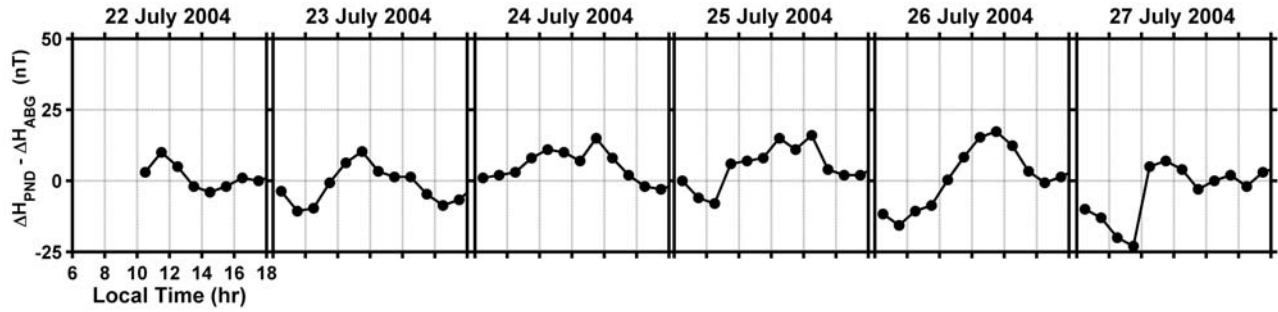


Figure 8. Daytime values of $\Delta H_{\text{Pondicherry}} - \Delta H_{\text{Alilig}}$ during the period 22–27 July 2004 as an indicator of the latitudinal extension of the equatorial electrojet current system.

and -1.85 . Thus in the present observations, the nonexistence of small-scale irregularities and the absence of radar echoes appear to be related to the lower level of spectral energy at large scales (>100 m) and steeper spectral slope (-4) than those reported by others.

[22] For the generation of the low-latitude *E* region FAIs, which manifest type 2 radar echoes, plasma density gradient and relative motion between the electrons and ions is the possible sources of free energy. With regard to the differential drift, *Raghavarao et al.* [2002] argued that the occurrence of low-latitude *E* region FAIs, such as those observed by Gadanki radar, may be related to the day-to-day variation in the latitudinal distribution of electrojet current system. According to them, an eastward wind increasing with altitude, called a positive wind shear, produces whorls of westward currents and downward vertical electric field at latitudes of Gadanki that inhibit the development of gradient drift instability, while the wind shears of negative polarity engender whorls of eastward currents and upward electric fields, which in turn cause the gradient drift instability.

[23] In an attempt to examine whether the latitudinal distribution of electrojet current system is anyway responsible for the daytime radar observations at Gadanki as pointed out by *Raghavarao et al.* [2002], we examined magnetometer observations from Pondicherry (11.92°N , 79.92°E , magnetic latitude 4.8°N) and Alilig (18.63°N , 72.87°E , magnetic latitude 10.02°N). Figure 8 shows $\Delta H_{\text{Pondicherry}} - \Delta H_{\text{Alilig}}$ as a measure of current over Pondicherry. Note that the ΔH values are well below 15 nT and thus are not significant. Also, we could not find any close correspondence between the ΔH variations and radar observations. Thus it appears unlikely that the latitudinal distribution of the electrojet current system would influence the occurrence/non-occurrence of radar echoes at Gadanki.

[24] On the other hand we have clearly shown that the radar echoing layers display descending behavior very similar to those of tidal winds. E_s also showed similar behavior. As far as the E_s layers are concerned, they are formed by the converging vertical ion motion due to wind shear [*Whitehead*, 1961]. According to the wind shear theory, the vertical ion velocity (w) can be written as

$$w = \frac{rUCos(I) + VSin(I)Cos(I)}{1 + r^2} \quad (1)$$

where U and V are zonal (eastward positive) and meridional (southward positive) winds, respectively, I is the dip angle

(13° at Gadanki), $r = \nu_i/\omega_i$, ratio of the ion-neutral collision frequency to gyrofrequency. For altitudes below 120 km, where r is greater than 1, the first term is more important than the second term in equation (1). Also the term “Sin I ” reduces the importance of the second term in equation (1). Hence the ion velocity can be simplified as:

$$w = \frac{rUCos(I)}{1 + r^2} \quad (2)$$

The above equation suggests that ion velocity is directly proportional to wind magnitude and inversely proportional to r (we can approximate $r/1 + r^2 \approx 1/r$). This means that for a given magnitude of wind, the efficiency decreases with decreasing altitude. Ideally, zonal wind shear with westward wind above and eastward wind below would converge the ions efficiently to form a layer. However, since the efficiency of the wind in converging ions decreases with decreasing altitude, the westward wind decreasing with altitudes and capable of providing necessary shear would be adequate enough for the ion layer formation. When the wind magnitude is higher than an instability threshold, the same wind generates small-scale irregularities [*Kagan and Kelley*, 1998]. The mechanism proposed by *Kagan and Kelley* [1998] further suggests that when the eastward wind is also present and strong enough, both sides of an E_s layer could be structured. In another study, *Kagan and Kelley* [2000] showed that if the zonal wind is strong enough it could generate plasma irregularities even without sporadic ionization layer by thermal instability. All these essentially advocate that strong zonal wind plays crucial role in the formation of plasma irregularities. The descent rates in radar echoing regions and E_s in the current observations, however, suggest the involvement of E_s layers in generating the plasma irregularities.

[25] In an effort to examine this aspect, we consider the TIMED Doppler Interferometry (TIDI) measured winds for the period of 22–27 July 2004. Figure 9a shows the wind profiles observed on 22, 24, 25, and 27 July. The profiles corresponding to the times when radar echoes were observed. These observations correspond to 15.53°N latitude (which is only 2° higher than that of Gadanki (13.5°N)) and 72.2° – 85.07°E longitudes (which are within $\pm 7^\circ$ of Gadanki longitude (79.2°E)). The wind profiles (eastward positive) show westward component corresponding to the height of radar echoes, which is the required wind direction for the E_s layer formation. Figure 9b shows two wind

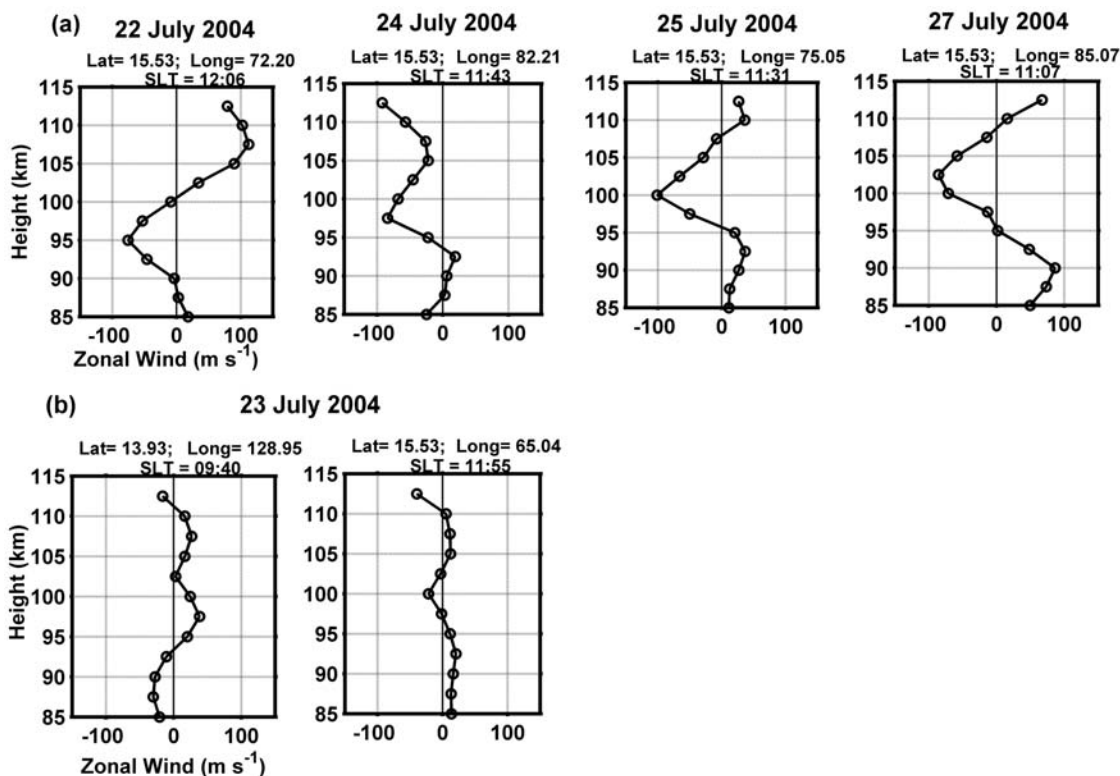


Figure 9. Height profiles of zonal wind observed by TIDI on (a) 22, 24, 25, and 27 July 2004 when radar echoes were observed and (b) 23 July 2004 when radar echoes were not observed.

profiles observed on 23 July corresponding to the times when radar echoes were absent. In this case, however, we could get TIDI wind profiles corresponding to longitudes of 65.04°E and 128.95°E , which are separated by $\sim 14^{\circ}$ and $\sim 50^{\circ}$ from Gadanki longitude. Both profiles show small values of wind whether it is eastward or westward. It is interesting to note that even though the two measurements correspond to locations separated by 63° and with respect to Gadanki one location is toward west and another toward east, the profiles are qualitatively similar in terms of their low wind magnitude. On this day, radar echoes were not observed for 4 h (0920–1320 LT) and the times of the two wind profiles happen to fall in this broad time sector. It is quite likely that such winds were responsible for not forming sharp electron density layer required for the manifestation of strong plasma irregularities, which is in agreement with the rocket, radar and ionosonde observations. Thus the observations seem to suggest that zonal winds play an important role in providing required electron density gradient through layer formation, which turns unstable presumably by gradient drift instability and eventually give rise to small-scale irregularities responsible for the radar echoes. Further investigation using more wind measurements and radar observations are essential to clarify the true role of the winds in the generation of low-latitude daytime *E* region plasma irregularities.

5. Concluding Remarks

[26] This investigation suggests that zonal wind plays an important role in the generation of the off-electrojet low-

latitude *E* region irregularities. It helps in forming sharp electron density layer, which subsequently becomes unstable via the gradient drift instability with background electric field or/and zonal neutral wind to generate plasma density irregularities. Further, we find that blanketing E_s is not an essential condition for the occurrence of low-latitude plasma irregularities observed by radar as hypothesized by *Krishnamurthy et al.* [1998]. We also find that the latitudinal distribution of electrojet current system over Gadanki is not a critical factor determining the day-to-day variability in the noontime occurrence of Gadanki radar echoes as hypothesized earlier by *Raghavarao et al.* [2002]. In view of the above, it would be interesting to evaluate the Piura radar observations of the daytime *E* region irregularities in terms of neutral winds and the characteristics of E_s layers, which would explain the difference between the daytime features of the low-latitude irregularities over Gadanki and Piura.

[27] **Acknowledgments.** Authors wholeheartedly appreciate the efforts made by the RSR group of VSSC, Trivandrum, and SDSC, Sriharikota, for payload integration and necessary launch support and the NARL technical team for successfully conducting the experiments with the MST radar. The rocket experiments were supported by ISRO. Magnetometer and wind data provided by IIG and TIDI team, respectively, through their Web sites are gratefully acknowledged. Authors gratefully acknowledge both the reviewers for their valuable suggestions, which improved the paper significantly.

[28] Amitava Bhattacharjee thanks Raj Kumar Choudhary for his assistance in evaluating this paper.

References

Chandra, H., H. S. S. Sinha, U. Das, R. N. Mishra, S. R. Das, J. Datta, S. C. Chakravarty, A. K. Patra, N. Venkateswara Rao, and D. Narayana Rao

- (2008), First mesospheric turbulence study using coordinated rocket and MST radar measurements over Indian low latitude region, *Ann. Geophys.*, *26*, 2725–2738.
- Chau, J. L., R. F. Woodman, and L. A. Flores (2002), Statistical characteristics of low latitude ionospheric field-aligned irregularities obtained with the Piura VHF radar, *Ann. Geophys.*, *20*, 1203–1212.
- Choudhary, R. K., K. K. Mahajan, S. Singh, and V. K. Anandan (1996), First VHF radar observations of tropical latitude *E* region field aligned irregularities, *Geophys. Res. Lett.*, *23*, 3683–3686, doi:10.1029/96GL02625.
- Hysell, D. L., M. C. Kelley, W. E. Swartz, and D. T. Farley (1994), VHF radar and rocket observations of equatorial spread F on Kwajalein, *J. Geophys. Res.*, *99*, 15,065–15,085, doi:10.1029/94JA00476.
- Kagan, L., and M. C. Kelley (1998), A wind driven gradient drift mechanism for mid-latitude *E* region ionospheric irregularities, *Geophys. Res. Lett.*, *25*, 4141–4144, doi:10.1029/1998GL900123.
- Kagan, L., and M. C. Kelley (2000), A thermal mechanism for generation of type-2 small-scale irregularities in the ionospheric *E* region, *J. Geophys. Res.*, *105*, 5291–5303, doi:10.1029/1999JA900415.
- Kelley, M. C., and R. Livingston (2003), Barium cloud striations revisited, *J. Geophys. Res.*, *108*(A1), 1044, doi:10.1029/2002JA009412.
- Kelley, M. C., W. E. Swartz, and J. Makela (2004), Mid-latitude ionospheric fluctuation spectra due to secondary $E \times B$ instabilities, *J. Atmos. Sol. Terr. Phys.*, *66*, 1559–1565, doi:10.1016/j.jastp.2004.07.004.
- Krishnamurthy, B. V., S. Ravindran, K. S. Viswanathan, K. S. V. Subbarao, A. K. Patra, and P. B. Rao (1998), Small-scale (~ 3 m) *E* region irregularities at and off the magnetic equator, *J. Geophys. Res.*, *103*, 20,761–20,773, doi:10.1029/98JA00928.
- Maruyama, T., S. Saito, M. Yamamoto, and S. Fukao (2006), Simultaneous observation of sporadic E with a rapid-rum ionosonde and VHF coherent backscatter radar, *Ann. Geophys.*, *24*, 153–162.
- Mathews, J. D., and F. S. Bekey (1979), Upper atmospheric tides and the vertical motion of ionospheric sporadic layers at Arecibo, *J. Geophys. Res.*, *84*, 2743–2750, doi:10.1029/JA084iA06p02743.
- Mori, H., and K. Oyama (1998), Sounding rocket observation of sporadic *E* layer electron-density irregularities, *Geophys. Res. Lett.*, *25*, 1785–1788, doi:10.1029/98GL00862.
- Patra, A. K., S. Sripathi, V. Sivakumar, and P. B. Rao (2002), Evidence of kilometre-scale waves in the lower *E* region from high resolution VHF radar observations over Gadanki, *Geophys. Res. Lett.*, *29*(10), 1499, doi:10.1029/2001GL013340.
- Patra, A. K., S. Sripathi, V. Sivakumar, and P. B. Rao (2004), Statistical characteristics of VHF radar observations of low latitude *E* region irregularities over Gadanki, *J. Atmos. Sol. Terr. Phys.*, *66*, 1615–1626, doi:10.1016/j.jastp.2004.07.032.
- Patra, A. K., S. Sripathi, P. B. Rao, and K. S. V. Subbarao (2005), Simultaneous VHF radar backscatter and ionosonde observations of low-latitude *E* region, *Ann. Geophys.*, *23*, 773–779.
- Prakash, S., and B. H. Subbaraya (1967), Langmuir Probe for the measurement of electron density and electron temperature in the ionosphere, *Rev. Sci. Instrum.*, *38*(8), 1132–1136, doi:10.1063/1.1721035.
- Raghavarao, R., A. K. Patra, and S. Sripathi (2002), Equatorial *E* region irregularities: A review of recent observations, *J. Atmos. Sol. Terr. Phys.*, *64*, 1435–1443, doi:10.1016/S1364-6826(02)00107-4.
- Whitehead, J. D. (1961), The formation of sporadic *E* layer in the temperate zones, *J. Atmos. Terr. Phys.*, *20*, 49–58, doi:10.1016/0021-9169(61)90097-6.
- Woodman, R. F., J. L. Chau, F. Aquino, R. R. Rodriguez, and L. A. Flores (1999), Low-latitude field-aligned irregularities observed in the *E* region with the Piura VHF radar: First results, *Radio Sci.*, *34*, 983–990, doi:10.1029/1999RS900027.

H. Chandra, U. Das, and H. S. S. Sinha, Physical Research Laboratory, Ahmedabad, 380009, India.

T. K. Pant, Space Physics Laboratory, VSSC, Trivandrum, 659022, India.

A. K. Patra and N. Venkateswara Rao, National Atmospheric Research Laboratory, Gadanki, 517112, India. (akpatra@narl.gov.in)

D. V. Phanikumar, Korea Astronomy and Space Science Institute, Daejeon, 305-348 South Korea.

S. Sripathi, Indian Institute of Geomagnetism, Panvel, Navi Mumbai, 410218, India.